J Mater Sci: Mater Electron
DOI 10.1007/s10854-013-1237-8

REVIEW

Structural transition of ZnO thin films produced by RF magnetron sputtering at low temperatures

A. M. Rosa · E. P. da Silva · M. Chaves · L. D. Trino · P. N. Lisboa-Filho · T. F. da Silva · S. F. Durrant · J. R. R. Bortoleto

Received: 18 January 2013 / Accepted: 12 April 2013

Abstract Zinc oxide (ZnO) thin films were prepared using reactive radio-frequency magnetron sputtering of a pure metallic zinc target onto glass substrates. The evolution of the surface morphology and the optical properties of the films were studied as a function of the substrate temperature, which was varied from 50 to 250 °C. The surface topography of the samples was examined using atomic force microscopy (AFM), and their optical properties were studied via transmittance measurements in the UV–Vis–NIR region. DRX and AFM analyses showed that the surface morphology undergoes a structural transition at substrate temperatures of around 150 °C. Actually, at 50 °C the formation of small grains was observed while at 250 °C the grains observed were larger and had more irregular shapes. The optical gap remained constant at ~3.3 eV for all films. In the visible region, the average optical transmittance was 80 %. From these results, one can conclude that the morphological properties of the ZnO thin films were more greatly affected by the substrate temperature, due to mis-orientation of polycrystalline grains, than were the optical properties.

A. M. Rosa · E. P. da Silva · M. Chaves · S. F. Durrant · J. R. R. Bortoleto (✉)
Laboratory of Technological Plasmas, São Paulo State University (UNESP), Av. 3 de Março, 511, Sorocaba, SP, Brazil
e-mail: jrborto@sorocaba.unesp.br

L. D. Trino · P. N. Lisboa-Filho
Group of Advanced Materials, São Paulo State University (UNESP), Av. Eng. Luiz Edmundo Carrijo Coube, 14-01, Bauru, SP, Brazil

T. F. da Silva
Laboratory of Materials Analysis with Ion Beams, São Paulo University (USP), Rua do Matão, trav. R, 187, São Paulo, SP, Brazil

1 Introduction

Zinc oxide (ZnO) is versatile material since it is an n-type semiconductor that belongs to the II–VI binary compounds, has a wide direct band gap of 3.3 eV at room temperature, and possesses a large exciton binding energy of ~60 meV [1, 2]. Moreover, ZnO has other attractive features such as reflectivity in the infrared region, good chemical stability, and high transparency in the visible region [2, 3]. These features make ZnO well-suited for many optoelectronic and piezoelectric applications such as solar cells, flat displays, chemical sensors and optical wave guides [4]. Owing mainly to its low cost, non-toxicity and the abundance of the chemical elements Zn and O in nature, ZnO is a promising alternative to indium tin oxide (ITO) in transparent conducting oxide (TCO) applications [1–5].

Zinc oxide thin films may be synthesized by a wide variety of techniques, including chemical and physical routes, such as pulsed laser deposition [6], thermal evaporation [7], chemical vapor deposition [8], electron beam evaporation [7], spray pyrolysis [9], sol–gel method [4] and magnetron sputtering on a variety of substrates [10–13]. Owing to its high deposition rate, relative simplicity, and the typically good adhesion of the film to the substrate [14], sputtering is the most promising method for depositing ZnO films Of particular note, deposition by magnetron sputtering allows the synthesis of ZnO films at low temperatures, which allows the use of flexible substrates, such as polymers, that can not support high temperatures.

The characteristics of ZnO films are usually affected by intrinsic and extrinsic factors, such as the pressure during deposition, the type of substrate, the film thickness and the substrate temperature [1, 2, 14]. The latter parameter is particularly important. In this study, ZnO films were deposited onto glass substrates by reactive RF magnetron

Published online: 07 May 2013

sputtering using a zinc metallic target at relatively low temperatures. The effects of substrate temperature on the structural, morphological and optical properties of the ZnO films were investigated.

2 Experimental procedure

ZnO films were deposited onto glass and silicon substrates in the same batch using reactive RF magnetron sputtering. A metallic zinc target of 76.2 mm diameter and 99.99 % purity was used as the zinc source. The target to substrate distance was 40 mm. Gas flows were controlled using needle valves and a mass flow controller. The plasma was activated by a 13.56 MHz RF power of 70 W at an argon pressure of 1.0×10^{-2} Torr and an oxygen flow rate of 0.08 sccm. Before each deposition, the target was sputtered with argon and oxygen for 10 min to remove the native oxide layer. Depositions were carried out at different substrate temperatures, ranging from 50 to 250 °C. The temperature was controlled during the deposition process such that the maximum fluctuations were ±5 °C. A constant deposition time of 60 min was used.

The surface topography of the samples was measured using atomic force microscopy (AFM, XE-100, Park Systems) operating in non-contact mode with a silicon cantilever (nominal radius of 10 nm). An area of 2×2 μm^2 was scanned at a resolution of 512 × 512 pixels. From the AFM measurements, the surface roughness was quantified using the root mean square (*rms*) roughness, σ, and the lateral correlation length, ξ (average lateral grain size). The optical transmittance of the films was measured using a UV–Vis–NIR spectrometer (Lambda 750, Perkin Elmer). Transmittance spectra were used to estimate the film thickness, optical energy gap (E_g) and the average optical transmittance. The crystallite orientation and grain size of the ZnO films were measured using an X-ray diffractometer system (D/MAX-2100/PC, Rigaku), which employs the Cu K_α radiation (1.54056 Å) at grazing incidence (3°). The chemical composition and density of films deposited onto silicon substrates were obtained by Rutherford backscattering spectroscopy (RBS) with 2.2 MeV He ions. A scanning electron microscope (SEM, XL-30, Philips FEG) was used to image the surface of the ZnO films.

3 Results and discussion

3.1 Film composition

Table 1 shows the deposition rate and compositions of the ZnO films produced at different substrate temperatures. As expected, the growth rate has a negative correlation with the substrate temperature, since the Zn desorption on the growing surface rises as the substrate heats, resulting in a lower growth rate [15].

The composition of the ZnO films was determined by RBS. The Zn atomic composition was greater than the O atomic composition irrespective of the substrate temperature, and all films were nearly stoichiometric (O/Zn ratio $\approx$1.00). In fact, it was also found that the O/Zn atomic ratio decreased slightly upon increasing the substrate temperature from 100 to 250 °C. These results indicate that the sputtered conditions used here were in the metal-to-oxide transition mode [5]. The Zn desorption is counterbalanced by the O_2 partial pressure at the sample holder, keeping the ZnO stoichiometry almost fixed.

3.2 Structural studies

Film density was calculated using the surface density measured by RBS and the film thickness measured from the respective transmittance spectra. These results are summarized in Table 1 as a function of the substrate temperature. In the temperature range from 50 to 150 °C, the density of the films increases with increasing substrate temperature. At substrate temperatures above 150 °C, however, the density starts to drop with increasing substrate temperature. Thus, the compactness of the film structures increases with increasing substrate temperature in the range of 50–150 °C, resulting in films with less porous structures. For substrate temperatures of 200 and 250 °C, the films are less compact, which indicates an increase in the density of voids in the ZnO film structure.

Figure 1 presents the X-ray diffraction pattern for ZnO films produced at different substrate temperatures. It can be observed that all the characteristic peaks of hexagonal ZnO wurtzite (according to JCPDS 65-3411), are present. Furthermore, the peaks indicate that the films are polycrystalline [16]. Strong (002) diffraction peaks are observed for all the films. These features indicate that the textured structure of these ZnO films grows with a preferential orientation along the *c* axis, perpendicular to the substrate surface [16]. The ZnO films grown at substrate temperatures of 200 and 250 °C show multiple reflections [(100) and (101) peaks], but with a dominant (002) peak. Singh et al. [11] studied the influence of substrate temperature on the structural properties of ZnO thin films, describing the same behavior for films deposited at substrate temperatures in the 150–250 °C range.

As can be observed from Fig. 1, the intensity of the (002) peak decreases monotonically with increasing substrate temperature. According to Lin et al. [14], the (002) peak intensity decreases with substrate temperature due to non-stoichiometric oxygen, which increases the defect level in the ZnO layer. A similar argument is proposed by

Table 1 Growth rate, composition, atomic density and optical properties of the ZnO films as a function of the substrate temperature

Substrate temperature (°C)	Growth rate (nm/min)	Zn (at.%)	O (at.%)	O/Zn	Density ($\times 10^{22}$ at./cm^3)	E_g (eV)	Average transmittance (%)
50	12.5	50.6	49.4	0.98	9.2	3.28	81.1
100	12.5	50.1	49.9	1.00	10.0	3.28	80.9
150	11.2	51.2	48.8	0.95	10.2	3.29	82.8
200	9.9	51.4	48.6	0.95	8.0	3.27	81.0
250	9.5	51.6	48.4	0.94	7.1	3.27	73.5

The errors in the composition and atomic density were estimated to be ±0.5 and 1 %, respectively

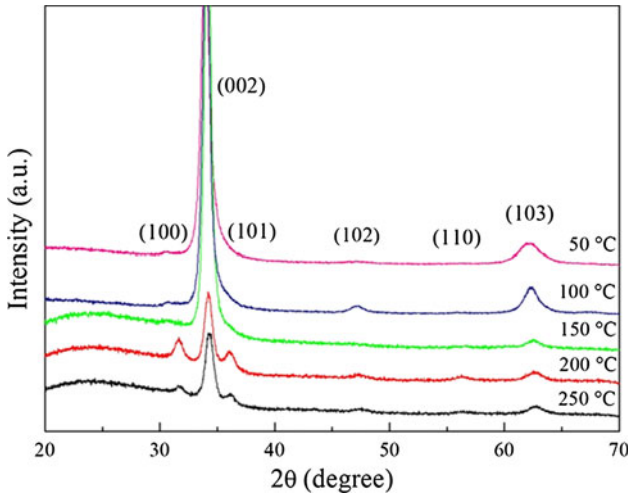

Fig. 1 XRD patterns of ZnO films deposited at different substrate temperatures

Yuste et al. [2] to explain the change in the oxygen partial pressure. In our case, however, the O/Zn ratio varies weakly between 1.00 and 0.94 in the range of temperature investigated, rather than between 1.00 and 0.65 as observed by Lin et al. This implies that the proposed mechanism may be negligible in the production of our films. On the other hand, the reduction in the (002) peak intensity may be related to mis-orientation of (002) planes with the substrate surface as reported by Singh et al. [11]. The disorientation of the planes tends to increase the presence of voids in the structure of the films, which is coherent with the reduction of the density of the ZnO films discussed above.

According to the XRD patterns of the films, there are shifts in the position of the (002) peaks at greater substrate temperatures. The position of the (002) peak changes from 34° for the film deposited at 50 °C to 34.32° for the film deposited at 250 °C, the latter being quite close to the value for 34.42° of bulk ZnO (JCPDS 65-3411). This indicates that the films suffered compressive stress at greater substrate temperatures. The lattice constant c was obtained from the position of the (002) peak for all films, and was used to estimate the strain (ε) in the films along the c axis as given by $\varepsilon = (c_{film} - c_{bulk})/c_{bulk}$ [11]. Figure 2a displays the variation of the strain with increasing substrate temperature. The decrease in strain may be attributed to annealing effects, resulting in the reduction of defects as related by Singh et al. [11].

The FWHM of the strongest (002) peak in Fig. 1 was used to estimate the crystallite size along the growth direction by employing Scherrer's relation [13]. Figure 2b shows the variation of the crystallite size with substrate temperature. It can be observed that in the films deposited at up to 100 °C, the crystallite size along the c axis increases from 9 to ~12 nm. A brief decline is seen in crystallite size for films deposited in the temperature range of 150–250 °C, which simultaneously exhibited a decrease in the (002) peaks in the XRD spectra.

3.3 Surface morphology

Figure 3a, b shows scanning electron micrographs of the textured surface of the ZnO films deposited at 100 and 250 °C, respectively. Distinct surface structures of the two films are evident. Thus, for the film grown at 100 °C, the surface is formed by small rounded grains of regular shapes of estimated average grain size of ~(176 ± 0.15 nm). On

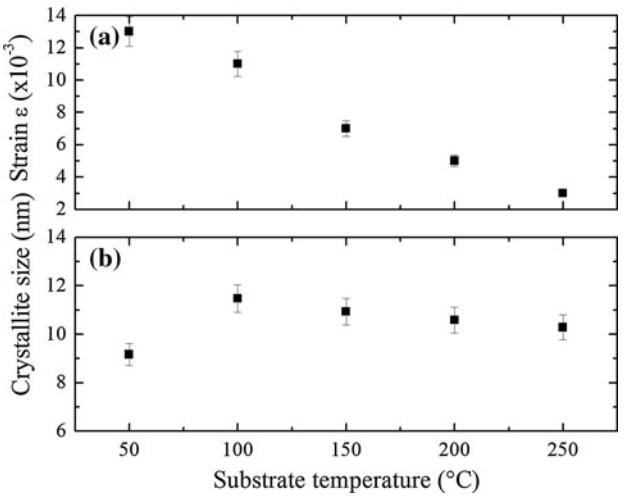

Fig. 2 **a** Strain of ZnO films and **b** grain size along c-axis (growth direction) as a function of the substrate temperature

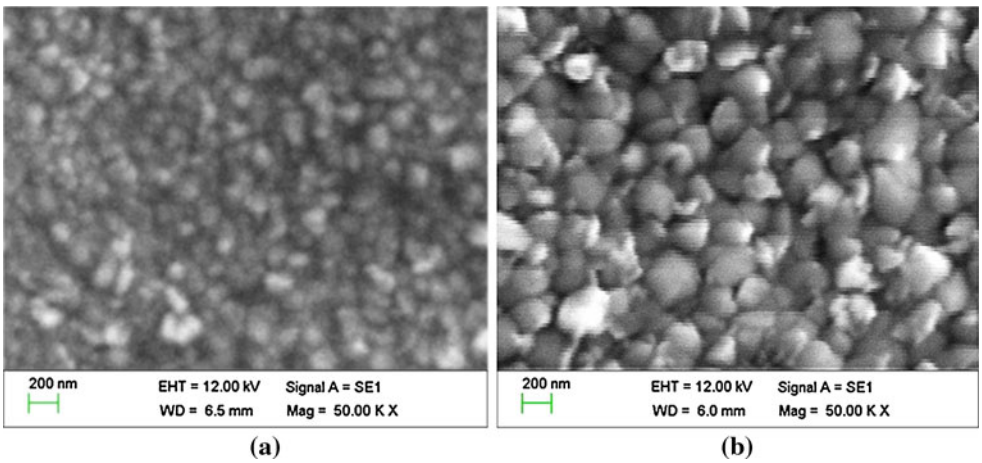

Fig. 3 The scanning electron micrograph of the surface textured of ZnO film deposited at **a** 100 and **b** 250 °C

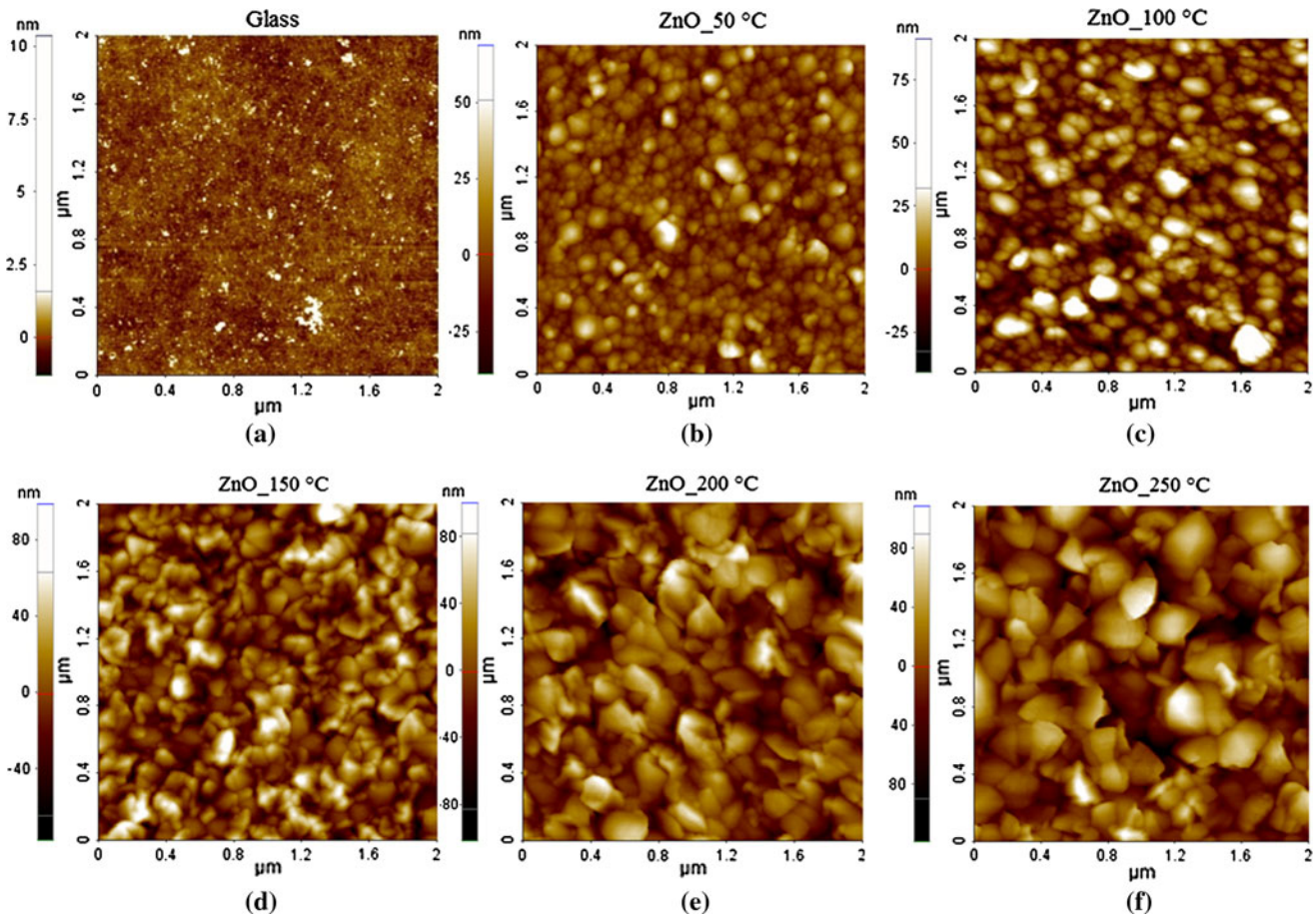

Fig. 4 2 × 2 µm AFM images of glass substrate and ZnO films deposited at different substrate temperatures. **a** Glass substrate, **b** 50 °C, **c** 100 °C, **d** 150 °C, **e** 200 °C and **f** 250 °C

the other hand, the film grown at 250 °C presents larger grains and has irregular shapes of estimated average grain size of ∼(351 ± 0.38 nm). In thin films, the morphologies of growth fronts and their evolution reflect the microscopic growth dynamics. Typically, film growth is a process far from equilibrium that can lead to the evolution of nanostructures on the front surface [16], resulting in a textured surface [14].

The surface morphology of the ZnO films was investigated using the AFM images shown in Fig. 4a–f. These

images show two-dimensional AFM images of the glass substrate and ZnO films grown at substrate temperatures of 50–250 °C, respectively.

All images show polycrystalline structures in which the lateral correlation length ξ, increases with increasing substrate temperature, as shown in Fig. 5a. In Fig. 4b, c, which correspond to substrate temperatures of 50 and 100 °C, respectively, the surface features are formed by small, regular grains with ξ in the range of 60–70 nm. In contrast, as the temperature of the substrate increases, there is the formation of distinct surface structures as can be seen in Fig. 4e, f. The film deposited at 150 °C (Fig. 4e) shows a textured morphology formed by irregular sized grains with a ξ of 70 nm. A similar textured surface morphology was also formed on ZnO films as reported by Lin et al. [14] who related the effects of RF power and substrate temperature to the film properties. The films deposited at 200 and 250 °C have similar surface features which are still formed of irregular-sized grains, but greater than those observed in the films subjected to 150 °C, and with a ξ of 85–95 nm. Singh et al. [11] indicate that the increase in ξ of the morphological features is attributable to the increase in the lateral size of the crystallites.

Figure 5b shows the evolution of the *rms* surface roughness σ of the ZnO films with increasing substrate temperature. The roughness σ increases from 12 to 31.5 nm almost linearly with increasing substrate temperature. Similar behavior was reported by Lin et al. [14] for ZnO films grown at different substrate temperature. Thus, the grain grows continuously in lateral size and height.

3.4 Optical properties

The optical transmittance measurements for the ZnO films at different substrate temperatures are shown in Fig. 6a. All the films presented high transmittance with an average transmittance of 80 % in the visible region (450–650 nm). Singh et al. [11] studied the influence of substrate temperature on the optical properties of ZnO thin films, obtaining similar results. Ondo-Ndong et al. [10] analyzed the influence of RF power on sputtered ZnO films, finding an average transmittance of 88 % in the visible region. The sharp fall in transmittance below 400 nm results from the onset of fundamental absorption in ZnO [11].

Another parameter important for optoelectronic applications is the band gap [5]. Paraguay et al. [18] indicated that ZnO films have a direct band gap. Thus, the absorption edge for direct interband transitions is given by $\alpha h\nu = C\ (h\nu - E_g)^{1/2}$, where C is a constant for a direct transition and α is the optical absorption coefficient [14, 19]. The optical band gap energy can be obtained from extrapolation of the linear portion to the intercept graphs of $(\alpha E)^2$ versus $h\nu$. Figure 6b shows the plots of $(\alpha E)^2$ versus $h\nu$ for the ZnO films deposited at different substrate

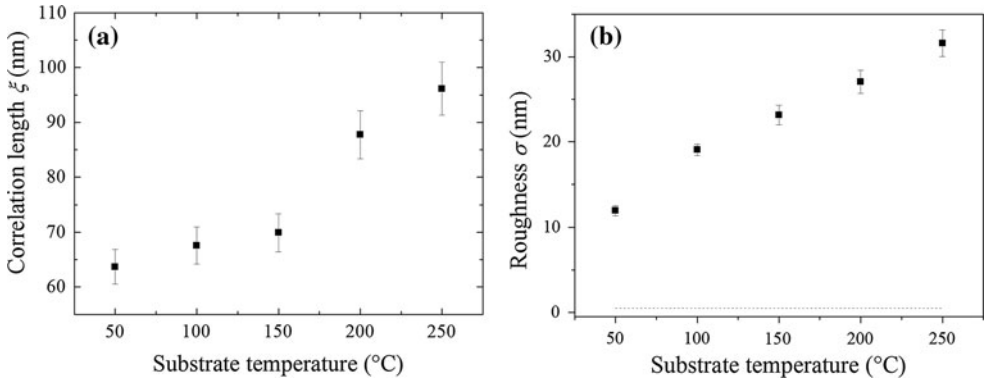

Fig. 5 **a** Lateral correlation length ξ calculated from the AFM images of ZnO films, which correspond to the average lateral grain size. **b** The surface roughness σ as a function of the substrate temperature as determined from 2 × 2 μm AFM images. The *dashed line* is the surface roughness of the glass substrate (~0.5 nm)

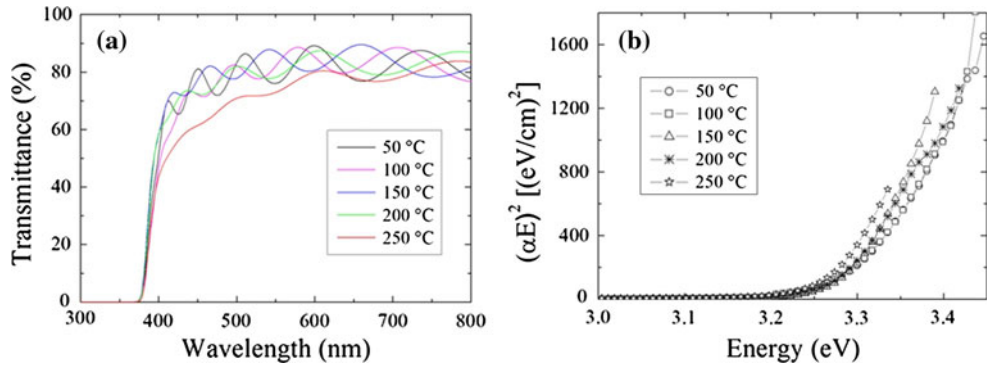

Fig. 6 **a** The optical transmittance spectra of the ZnO films deposited on glass substrates for different substrate temperatures. **b** The energy gap of the ZnO films estimated by the extrapolation of the linear part of the $(\alpha E)^2$ versus $h\nu$ plots

temperatures. Thus, for all the films, the band gaps found were approximately ~3.3 eV. This value is in agreement with the results reported in the literature [14–18].

Figure 6a shows the formation of exponential band tails, which is the decreasing slope of the transmission edge in the UV spectral range. Figure 6b shows a low energy tail. These tails may be explained by the existence of structural defects and impurities within the material [5, 19]. From Fig. 6b is observed at greater substrate temperatures, the plots of $(\alpha E)^2$ as a function of hv become more straightforward. According to Singh et al. [11], this can occur due to a reduction of defects in the films.

4 Conclusions

The effect of substrate temperature on the morphological and optical properties of ZnO thin films deposited by reactive RF magnetron sputtering onto glass substrates was investigated. ZnO films studied here are almost stoichiometric, although the Zn desorption rate is not negligible at higher temperatures. Moreover, all films exhibit an average transmittance of 80 % in the visible region and present band gaps of about 3.3 eV. At temperatures lower than 150 °C, the films are polycrystalline and exhibit a strong oriented growth along the (002) plane, perpendicular to the substrate surface. For temperatures higher than 150 °C, polycrystalline grains tend to grow mis-oriented and, as a consequence, the film density decreases. Moreover, the surface morphology changes abruptly as a function of the substrate temperature, resulting in grains with irregular shapes at temperatures greater than 150 °C. Finally, we can point out that the films deposited at 100–150 °C range, which corresponds to the maximum film density, are more suitable for TCO applications.

Acknowledgments The financial support of the Brazilian agencies FAPESP (Proc. 2008/53311-5) and CNPq is gratefully acknowledged.

References

1. K. Ellmer, in *Handbook of Transparent Conductors*, ed. by D.S. Ginley, H. Hosono, D.C. Painechap. Transparent conductive zinc oxide and its derivatives, 1st edn (Springer, Berlin, 2011)
2. M. Yuste, R. Escobar Galindo, I. Caretti, R. Torres, O. Sanchez, J. Phys. D Appl. Phys. **45**, 025303 (2012)
3. S. Youssef, P. Combette, J. Podlecki, R.Al Asmar, A.S. Foucaran, Cryst. Growth Des. **9**, 1088–1094 (2009)
4. T. Kuchiyama, K. Yamamoto, S. Hasegawa, H. Asahi, Appl. Surf. Sci. **258**, 1488–1490 (2011)
5. Y.H. Jo, B.C. Mohanty, Y.S. Cho, J. Am. Ceram. Soc. **92**, 665–670 (2009)
6. E. Vasco, C. Zaldo, L. Vázquez, J. Phys.: Condens. Matter **13**, L663–L672 (2001)
7. W. Mtangi, F.D. Auret, P.J. Janse van Rensburg, S.M.M. Coelho, M.J. Legodi, J.M. Nel, W.E. Meyer, A. Chawanda, J. Appl. Phys. **110**, 094504 (2011)
8. Y.-S. Choi, D.-K. Hwang, B.-J. Kwon, J.-W. Kang, Y.-H. Cho, S.-J. Park, Jpn. J. Appl. Phys. **50**, 105502 (2011)
9. E. Sonmez, S. Aydin, M. Yilmaz, M.T. Yurtcan, T. Karacali, M. Ertugrul, J. Nanomater. **2012**, 05 (2011)
10. R. Ondo-Ndong, G. Ferblantier, M. Al Kalfioui, A. Boyer, A. Foucaran, J. Cryst. Growth **255**, 130–135 (2003)
11. S. Singh, R.S. Srinivasa, S.S. Major, Thin Solid Films **515**, 8718–8722 (2007)
12. H.F. Liu, S.J. Chua, G.X. Hu, H. Gong, N. Xiang, J. Appl. Phys. **102**, 083529 (2007)
13. C.-A. Tseng, J.-C. Lin, Y.-F. Chang, S.-D. Chyou, K.-C. Peng, Appl. Surf. Sci. **258**, 5996–6002 (2012)
14. S.-S. Lin, J.-L. Huang, D.-F. Lii, Surf. Coat. Technol. **176**, 173–181 (2004)
15. K. Koski, J. Hölsä, P. Juliet, Thin Solid Films **339**, 240 (1999)
16. Y. Kajikawa, J. Cryst. Growth **289**, 387–394 (2006)
17. R. Álvarez, A. Palmero, L.O. Prieto-López, F. Yubero, J. Cotrino, W. de la Cruz, H. Rudolph, F.H.P.M. Habraken, A.R. Gonzalez-Elipe, J. Appl. Phys. **107**, 054311 (2010)
18. F. Paraguay, W. Estrada, D.R. Acosta, E. Andrade, M. Miki-Yoshida, Thin Solid Films **350**, 192–202 (1999)
19. S.-S. Lin, J.L. Huang, Surf. Coat. Technol. **185**, 222–227 (2004)